Published in final edited form as:
Cell. 2014 July 17; 158(2): 300–313. doi:10.1016/j.cell.2014.04.050.

Crosstalk between Muscularis Macrophages and Enteric Neurons Regulates Gastrointestinal Motility

Paul Andrew Muller[1,2,3,&], **Balázs Koscsó**[7], **Gaurav Manohar Rajani**[7], **Korey Stevanovic**[8], **Marie-Luise Berres**[1,2,3], **Daigo Hashimoto**[1,2,3,#], **Arthur Mortha**[1,2,3], **Marylene Leboeuf**[1,2,3], **Xiu-Min Li**[5,6], **Daniel Mucida**[10], **E. Richard Stanley**[11], **Stephanie Dahan**[3,4], **Kara Gross Margolis**[8], **Michael David Gershon**[9], **Miriam Merad**[1,2,3,*], and **Milena Bogunovic**[1,2,3,7,*]

[1]Department of Oncological Sciences, Icahn School of Medicine at Mount Sinai Hospital, New York, NY 10029, USA

[2]The Tisch Cancer Institute, Icahn School of Medicine at Mount Sinai Hospital, New York, NY 10029, USA

[3]The Immunology Institute, Icahn School of Medicine at Mount Sinai Hospital, New York, NY 10029, USA

[4]Division of Clinical Immunology, Department of Medicine, Icahn School of Medicine at Mount Sinai Hospital, New York, NY 10029, USA

[5]Division of Allergy and Immunology, Department of Pediatrics, Icahn School of Medicine at Mount Sinai Hospital, New York, NY 10029, USA

[6]Jaffe Food Allergy Institute, Icahn School of Medicine at Mount Sinai Hospital, New York, NY 10029, USA

[7]Department of Microbiology and Immunology, Penn State University College of Medicine and Milton Hershey Medical Center, Hershey, PA 17033, USA

[8]Department of Pediatrics, Morgan Stanley Children's Hospital, Columbia University College of Physicians and Surgeons, New York, NY 10032, USA

CORRESPONDENCE: Milena Bogunovic, 500 University Drive, Hershey, PA 17033, USA, mbogunvich@mhc.psu.edu, **Miriam Merad**, 1470 Madison Avenue, New York, NY10029, USA, miriam.merad@mssm.edu.
[&]Laboratory of Mucosal Immunology, The Rockefeller University, New York, NY 10065, USA and The Sackler Institute of Graduate Biomedical Sciences, New York University School of Medicine, New York, NY 10016, USA
[#]Present address: Department of Hematology, Hokkaido University Graduate School of Medicine, N15 W7, Kita-Ku, Sapporo 060-8638, Japan
[*]These authors equally contributed to this work

AUTHOR CONTRIBUTIONS

P.M. designed, performed experiments and helped write the manuscript; M.B. led the project, designed and performed experiments and wrote the manuscript; M.M. initiated and led the project and helped write the manuscript; K.G.M. and M.D.G. provided intellectual input and helped write the manuscript; D.M. and X.-M.L. assisted with methodology; E.R.S. provided reagents; B.K., G.R., K.S., S.D., M.-L.B., D.H., A.M. and M.L. performed experiments.

COMPETING FINANCIAL INTERESTS

The authors declare no competing financial interests.

[9]Department of Pathology and Cell Biology, Columbia University College of Physicians and Surgeons, New York, NY 10032, USA

[10]Laboratory of Mucosal Immunology, The Rockefeller University, New York, NY 10065, USA

[11]Department of Developmental and Molecular Biology, Albert Einstein College of Medicine, Bronx, NY 10461, USA

SUMMARY

Intestinal peristalsis is a dynamic physiologic process influenced by dietary and microbial changes. It is tightly regulated by complex cellular interactions; however, our understanding of these controls is incomplete. A distinct population of macrophages is distributed in the intestinal muscularis externa. We demonstrate that in the steady state muscularis macrophages regulate peristaltic activity of the colon. They change the pattern of smooth muscle contractions by secreting bone morphogenetic protein 2 (BMP2), which activates BMP receptor (BMPR) expressed by enteric neurons. Enteric neurons, in turn, secrete colony stimulatory factor 1 (CSF1), a growth factor required for macrophage development. Finally, stimuli from microbial commensals regulate BMP2 expression by macrophages and CSF1 expression by enteric neurons. Our findings identify a plastic, microbiota-driven, crosstalk between muscularis macrophages and enteric neurons, which controls gastrointestinal motility.

INTRODUCTION

Peristaltic movements of the gut are essential to propel ingested material through the gastrointestinal (GI) tract. These movements are generated by coordinated contractions and relaxations of the circular and longitudinal smooth muscles that form the *muscularis externa* (Figure 1A). The pattern and frequency of peristaltic contractions are locally regulated by the enteric nervous system (ENS) (Furness, 2012) and pacemaker interstitial cells of Cajal (ICC) (Huizinga et al., 1995; Rumessen and Vanderwinden, 2003).

Mononuclear phagocytes, which include dendritic cells (DCs) and macrophages, form a heterogeneous group of myeloid cells found in most tissues. Their common functions are to maintain tissue homeostasis through scavenging and participation in immune responses (Hashimoto et al., 2011b). A network of $MHCII^{+}$ macrophages exists in the intestinal muscularis both in mice and humans (Mikkelsen and Rumessen, 1992; Mikkelsen et al., 1985). This network extends from the stomach to the distal colon (Mikkelsen, 2010). Within the muscularis, these macrophages mainly accumulate in layers, between the serosa and the longitudinal muscle, between longitudinal and circular muscles, and between the outer and inner circular muscles (Mikkelsen, 2010). In addition to their phagocytic properties (Mikkelsen et al., 1985), muscularis macrophages (MMs) are potent antigen-presenting cells and are sometimes referred to as DCs (Flores-Langarica et al., 2005).

The functions of MMs are far less defined compared to their mucosal counterparts. Some studies have implicated MMs in the pathogenesis of post-operative ileus, a transient inflammatory condition of the GI tract that results in intestinal paralysis (Mikkelsen, 2010). In surgically manipulated areas of the gut, the release of inflammatory mediators by

activated MMs is thought to impair GI motility by affecting smooth muscle contractility directly as well as through the recruitment of additional inflammatory cells (Boeckxstaens and de Jonge, 2009; Wehner et al., 2007). Whether MMs play a role in regulating constitutive gastrointestinal physiology, however, has never been determined. Intrigued by the distinctive distribution of these cells and driven by the idea that macrophages are essential regulators of tissue homeostasis (Chow et al., 2013; Chow et al., 2011; Wynn et al., 2013), we hypothesized that MMs may provide trophic support to smooth muscle cells and through that support regulate constitutive GI motility.

To test our hypothesis, we developed a model for the selective transient depletion of MMs. We then demonstrated that MMs regulate intestinal peristalsis at steady state and identified a specific factor, BMP2, secreted by MMs that regulates GI motility through a direct action, not on smooth muscle, but on enteric neurons. Our work revealed that MMs and enteric neurons communicate with each other. MMs support enteric neurons by providing BMP2, whereas neurons promote MM homeostasis through production of the macrophage-specific growth factor CSF1. Finally, we have found that signals from the intestinal microbiota are able to influence the crosstalk between MMs and enteric neurons and alter GI motility.

RESULTS

MM development requires CSF1 receptor signaling

The intestine is a complex layered structure that includes mucosa, submucosa and muscularis externa (Figure 1A). The intestinal mucosa is populated by two ($CD103^+CD11b^+CX_3CR1^-$ and $CD103^-CD11b^+$ CX_3CR1^+) prevalent subsets of mononuclear phagocytes, each with a different developmental pathway and function (Bogunovic et al., 2009; Bogunovic et al., 2012). Very little is known about the phenotype and function of MMs, mainly because these cells are difficult to isolate from intestinal tissue. A technique for separation of the intestinal muscularis externa from the overlying mucosa and submucosa allowed us to perform a detailed analysis of MMs using whole mount tissue preparations and single cell suspensions (Bogunovic et al., 2009). By combining flow cytometry and immunofluorescence analysis, we have shown that MMs represent a homogeneous population of $MHCII^{hi}CD11c^{lo}CD103^-CD11b^+$ cells (Bogunovic et al., 2009), which express high levels of CX_3CR1 (Figure 1A–C). The MM population resembles the $CD103^-CD11b^+CX_3CR1^+$ macrophages, which are found in the intestinal lamina propria (LP) (Bogunovic et al., 2009). In a suspension of intestinal cells, MMs can easily be distinguished from $CD11c^{hi}$ LP phagocytes by the lower expression of CD11c and higher expression of MHCII (Bogunovic et al., 2009) (Figure S1A).

FLT3 and CSF1 (also known as macrophage colony stimulatory factor, M-CSF) receptor (CSF1R) are two key growth factor receptors that control mononuclear phagocyte development (Hashimoto et al., 2011b). We have previously demonstrated that $CD103^-CD11b^+$ LP phagocytes require CSF1R signaling for their homeostasis and are reduced in *Csf1r*$^{-/-}$ mice (Bogunovic et al., 2009). The phenotypic similarity between MMs and $CD103^-CD11b^+$ LP phagocytes led us to investigate the role of CSF1R in MM development. We found that MMs express *Csf1r* (Figure 1D) and must absolutely be dependent on CSF1R signaling because *Csf1r*$^{-/-}$ mice lack these cells (Figure 1E–G).

Moreover, *Csf1r*$^{-/-}$ bone marrow progenitors fail to develop into MMs when transplanted into lethally irradiated recipients (Figure 1H).

To study the function of MMs we developed a model in which homeostatic properties are used to selectively deplete MMs. We found that MMs are more dependent on CSF1R signaling than LP phagocytes (Figure 1G–H), which provided us with a strategy to selectively deplete one population without affecting the other. Because CSF1R expression in the gut is restricted to MMs and mucosal macrophages (Figure S1B–D, small bowel mucosa and submucosa – not shown), a single intraperitoneal (i.p.) injection of a low dose of a blocking anti-CSF1R monoclonal antibody (Sudo et al., 1995) (αCSF1R mAb) was able to deplete at least 80% MMs (Figure 2A–E, S2A–B) without depleting LP phagocytes (Figure 2C–D, S2B) or stromal cells (not shown). MM numbers were reduced 24 hours after the antibody injection and returned to normal 7 days later (not shown). No differences in CSF1 levels in MMs and MM depletion efficiency were observed between the small and large bowel (Figure S1C, Figure 2A–E, Figure S2A–B). This depletion was considered to be non-inflammatory because there was no lymphocyte (Figure 2F, Figure S2C–D), neutrophil or monocyte (not shown) recruitment in either muscularis or mucosa. Injection of αCSF1R mAb also did not increase apoptotic cell numbers in the gut (Figure S2E). Taken together, these findings identified CSF1R as essential for MM development and established blocking CSF1R *in vivo* as a model for the transient depletion of these cells.

MMs regulate gastrointestinal motility at steady state

In the isolated intestine, the peristaltic reflex can be elicited by providing a distending force to the intestinal wall (Frigo and Lecchini, 1970). To determine whether conditional depletion of MMs affects the peristaltic reflex, we developed an *ex vivo* method to record peristaltic contractions in response to stepwise distension of colonic rings (Figure 3A). Repeated applications of increasing stretch resulted in an immediate contraction of the rings, followed by gradual relaxation creating a ladder-like pattern of recordings. Augmented stretching generated additional high amplitude contractions (further called “stretch-induced contractions”), which gradually increased in amplitude and frequency (Figure 3B). In MM depleted colonic rings stretch-induced contractions were evoked at shorter durations of stretch, were more rapid and had a significantly higher frequency (Figure 3B–C); thus the root mean square (RMS) of the signal was increased (Figure 3C–D). Despite the evident colonic hyper-reactivity *ex vivo*, colonic transit time, measured *in vivo* by bead expulsion assay, was increased after MM depletion, probably because muscle contractions were poorly coordinated and inefficient (Figure 3E). Among other parameters of GI motility gastric emptying was accelerated, whereas transit from stomach along the small bowel and total intestinal transit time were not significantly changed (Figure S2F–H). This would occur if accelerated gastric emptying and delayed small and large bowel motility cancel each other out thus suggesting that motility of the entire GI tract is affected by MM depletion.

To further confirm the role of MMs in regulating GI motility, we generated syngeneic bone marrow (BM) chimeric animals with *Csf1r*$^{-/-}$ hematopoietic progenitors (from fetal liver). Some *Csf1r*$^{-/-}$ BM chimeric mice clearly developed a delay of colonic transit time (Figure S2I); nevertheless, poor engraftment of *Csf1r*$^{-/-}$ BM and the consequent low survival rate of

these chimeric animals did not permit us to obtain enough animals for statistical comparisons.

In summary, the observation that removal of MMs results in dysmotility indicates that MMs contribute to the physiological regulation of GI motility.

MMs regulate intestinal peristalsis through the production of BMP2

These findings raised the question: by what mechanisms do MMs affect GI motility? We tested the initial hypothesis that MMs secrete a soluble factor that alters smooth muscle contractility. To identify the gene that encodes a putative target protein, we carried out a whole mouse genome microarray on different purified intestinal phagocyte subsets (Bogunovic et al., 2009; Bogunovic et al., 2012) and did a comparative data analysis to select genes highly expressed by MMs but not by related $CD103^{-}CD11b^{+}$ LP macrophages. Bone morphogenetic protein 2 (BMP2) was identified as the only non-immune gene among the "top four" (*Cd163*, *F13a1*, *Clec4e*, *Bmp2*) most highly expressed genes that also encoded a soluble factor (Figure 4A–B). No other BMP family members were expressed by either intestinal phagocyte subset (Figure 4C and not shown). BMPs are a group of secreted proteins in the TGF-b superfamily that are thought to mainly control organ development (Hogan, 1996). $Bmp2^{-/-}$ mice are embryonically lethal (Zhang and Bradley, 1996) and $Bmp2^{+/-}$ mice are susceptible to hypoxic pulmonary hypertension characterized by sustained high pressure in pulmonary arteries due to increased vascular reactivity and structural remodeling (Anderson et al., 2010). BMP2 is highly expressed in the fetal but not adult gut and BMP receptor (BMPR) signaling has been implicated in enteric smooth muscle and neuronal differentiation (Chalazonitis et al., 2004; Chalazonitis et al., 2011; Chalazonitis et al., 2008; Faure et al., 2007b; Fu et al., 2006; Goldstein et al., 2005). Using qPCR we confirmed that *Bmp2* is expressed in MMs but is absent in purified muscularis lymphocytes (Figure 4D). *In situ* BMP2 protein expression was also restricted to $MHCII^{+}$ MMs (Figure 4E). To examine whether BMP2 plays a role in regulating colonic motility we compared the pattern of stretch-induced contraction of colonic rings from mice treated *in vivo* with the inhibitor of BMPR signaling, dorsomorphin (Yu et al., 2008) to those treated only with vehicle. Treatment with dorsomorphin elicited a pattern of contractile hyper-reactivity similar to that seen in colonic rings from MM-depleted mice (Figure 4F; Figure S3A). To confirm that the pattern resulted from deficient BMPR signaling, we carried out a "rescue" experiment in which increasing concentrations of exogenous BMP2 were added to the colonic rings from MM-depleted mice. BMP2 was added during recording of stretch-induced contractions at a previously determined "optimal" 2.75 mm stretch distance. BMP2 reduced stretch-induced contractions in a concentration dependent manner (Figure 4 G-I). There were no changes in contractility when the same amounts of BMP2 were added to colonic rings in which MMs had not been depleted (Figure 4G). Consistent with our *in vitro* data, BMP2 injection partially accelerated colonic transit time (Figure 4J). Taken together, our data support the idea that MM secretion of BMP2 regulates colonic contractility.

MMs activate enteric neurons that express BMPR

We next sought to identify the cells targeted by MM-derived BMP2. The force with which smooth muscles contract in response to exogenous stimuli (stretch or KCl) was unaffected

after MM depletion (Figure S3B–C). CKit$^+$ ICC and βIII-Tubulin$^+$ ENS networks do not overlap (Figure S4A). Both ICC and ENS networks remained intact after MP depletion (Figure S3D; Fig. 5C), indicating that acute MM depletion does not anatomically disrupt ICCs or the ENS. The numbers of epithelial serotonin$^+$ enteroendocrine cells, which activate peristaltic reflexes in response to luminal signals (Bulbring and Crema, 1959a, b; Heredia et al., 2013), were also unaffected by injection of αCSF1R mAb (Figure S3E–F). Additionally, intestinal epithelial permeability remained unaffected even after the treatment with maximal doses of αCSF1R mAb (Figure S3G–H). We assessed the anatomical interaction between MMs and enteric neurons and found that the vast majority of MMs were positioned along nerve fibers, often forming close appositions (Figure 5A). BMP2 signals through the oligomerization of type I and type II serine kinases (BMPRIa and BMPRII, respectively), which form the BMPR (Kirsch et al., 2000). We found that BMPRII was selectively expressed by neurons, marked with antibodies to βIII-Tubulin (Figure 5B), but not by ICCs (cKit$^+$; Figure S4B) and ENS associated glia (GFAP$^+$; Figure S4C), suggesting that MMs act on enteric neurons. Ligand binding to BMPR activates the canonical signaling pathway through phosphorylation and nuclear translocation of SMADs 1, 5 and 8 (Derynck and Zhang, 2003). Treatment of cultured primary enteric neurons, which express *BmprIa* and *BmprII* but not *BmprIb* and *Bmp2* (Figure S4D), with recombinant BMP2 resulted in the rapid accumulation of pSMAD1/5/8 complex in the neuronal nuclei (Figure S4E); moreover, the nuclei of the vast majority of BMPRII$^+$ enteric neurons *in vivo* were positive for pSMAD1/5/8, demonstrating that activation through BMPR was constitutively occurring (Figure 5C–D). In contrast, MM depletion resulted in the disappearance of pSMAD1/5/8 from nuclei in most of enteric neurons *in vivo*, consistent with the key contribution of MMs to BMPR signaling (Figure 5C–D). Incubation of the muscularis layer devoid of MMs with exogenous BMP2 restored the numbers of enteric neurons with pSMAD1/5/8-immunoreactive nuclei to nearly normal levels (Figure 5C–D). These data imply that MMs provide continuous signaling to neurons through the secretion of BMP2, which activates the BMPR that they express.

Enteric neurons produce the macrophage growth factor CSF1

CSF1 and IL-34 are two alternative ligands that activate CSF1R (Lin et al., 2008; Yeung et al., 1987) and each of these cytokines have been implicated in the development of different mononuclear phagocyte populations (Greter et al., 2012; Hashimoto et al., 2011b; Wang et al., 2012). MMs do not express either *Csf1* or *Il34* (not shown) suggesting that CSF1 and IL-34 must be produced by a different cell population, possibly stromal cells. CSF1 and Il-34 are alternatively expressed by distinct subtypes of mature neurons in the postnatal brain (Nandi et al., 2012). We thus asked whether there is additional crosstalk between enteric neurons and MMs in which enteric neurons provide CSF1R ligands to MMs. We found that enteric neurons express *Csf1* but not *Il34* in culture (Figure 6A–B) and are the main source of CSF1 protein in the muscularis (Figure 6C). As expected, and consistent with an earlier report (Mikkelsen and Thuneberg, 1999), CSF1-deficient *Csf1*$^{op/op}$ mice almost completely lack MMs (Figure 6D–F). These results suggest that enteric neurons likely play a key role in the maintenance of MM homeostasis.

Osteoclast deficiency related bone defects including toothlessness (Wiktor-Jedrzejczak et al., 1991) and the significantly smaller size of *Csf1*$^{op/op}$ mice (Figure S5A) prevented us from analyzing GI motility in these animals. However, we observed that despite the smaller size of both the length and diameter of the *Csf1*$^{op/op}$-intestine (length of SB – 80% of WT (Huynh et al., 2009), length of LB – 80% of WT), the cecum of these animals was larger than of WT mice (Figure S5B), suggesting that GI motility is dysregulated in *Csf1*$^{op/op}$ mice. Consistent with our data using the transient MM depletion model, we found that the numbers of pSMAD1/5/8^{+} enteric neurons were significantly reduced in the colon of *Csf1*$^{op/op}$ mice compared to WT littermates (Figure 6G, Figure S5C). We also observed a significant increase of the total numbers of enteric neurons together with less organized architecture of the ENS in *Csf1*$^{op/op}$ mice (Figure 6H–I), suggesting the importance of MMs in ENS development. This observation is similar to the ENS of NSE-noggin mice, which overexpress the endogenous BMP inhibitor noggin under the control of neuron specific enolase (NSE) promoter (Chalazonitis et al., 2004; Chalazonitis et al., 2008).

Luminal microbiota regulate macrophage-neuronal crosstalk

Luminal microbiota appear to be essential for the normal regulation of intestinal motility and severe dysmotility has been described in germ-free rodents (Abrams and Bishop, 1967; Gustafsson et al., 1970) and in *Tlr4*$^{-/-}$ and *Myd88*$^{-/-}$ mice (Anitha et al., 2012). The mechanisms by which commensals regulate intestinal motility are poorly understood and may involve abnormalities of many different cell types. Slowing of GI motility in germ-free, antibiotic treated, *Tlr4*$^{-/-}$ and *Myd88*$^{-/-}$ mice is accompanied by an alteration in the phenotypic diversity of enteric neurons with reduced numbers of nitrergic neurons (Anitha et al., 2012). Whether MMs contribute to these regulatory processes is not known. Similar to published reports (Abrams and Bishop, 1967; Anitha et al., 2012; Gustafsson et al., 1970), we found that GI motility is grossly disturbed in mice treated with broad-spectrum antibiotics (Figure 7A, Figure S6A–B). Megacolon also occurs in these animals (Figure S7E) thus bead expulsion assay was not valuable in measuring colonic motility. Upon *ex vivo* analyses we found that colonic rings from antibiotic-treated mice displayed a pattern of contractile hyper-reactivity similar to that seen in colonic rings from MM-depleted or dorsomorphin treated mice (Figure 7B, Figure S6C). Strikingly, we found that antibiotic-treated mice expressed significantly less *Bmp2* compared to control mice (Figure 7C), suggesting that microbial commensals influence the interaction between MMs and enteric neurons. Consistently, the numbers of pSMAD1/5/8^{+} enteric neurons were significantly reduced in antibiotic-treated mice compared to littermate controls that received only water (Figure 7D, Figure S6D). We then questioned whether commensal signals can also regulate CSF1 production by enteric neurons. We found that addition of LPS to cultured primary enteric neurons increased their expression of *Csf1* (Figure 7E). Interestingly, culture of primary enteric neurons in the presence of exogenous BMP2 did not affect *Csf1* expression levels (not shown). Consistently, antibiotic treatment *in vivo* reduced *Csf1* expression in the colonic muscularis (Figure 7F) although the kinetics of *Csf1* reduction was slow and reached its minimum after 4 weeks of treatment (Figure S7A). In line with the reduction of *Csf1*, antibiotic treatment also resulted in a decrease of MM numbers (Figure 7G, S7B–C) with similar kinetics (Figure S7B). No reduction in the numbers of mucosal macrophages was observed during the course of antibiotic treatment (not shown). Additionally, the numbers of

$Gr1^{hi}$ blood monocytes that give rise to both mucosal macrophages (Bogunovic et al., 2009) and MMs (unpublished) were not affected, thus excluding an effect on myeloid cell development in the bone marrow (Figure S7D).

Microbiota-associated factors that influence GI motility include constituents of nutriment breakdown, byproducts of microbial metabolism and microbial cellular components like LPS (Reigstad and Kashyap, 2013). While cecum enlargement was an early sign of antibiotic treatment, cecum size continued to increase over the course of treatment (Figure S7E) implying that various microbiota-associated factors contribute to antibiotic-induced dysmotility with different kinetics. The kinetics of reduction in *Csf1* expression and MM numbers was delayed as compared to the reduction of bacteria in the gut lumen during the antibiotic treatment (Figure S7F), suggesting that a decrease in serum LPS after prolonged antibiotic treatment (Anitha et al., 2012) might be responsible for those changes. To test this, mice were supplemented with LPS in drinking water as described (Rakoff-Nahoum et al., 2004) while maintained on antibiotics. Consistent with the *in vitro* data and our hypothesis, LPS supplementation prevented the reduction of *Csf1* expression and MM numbers (Figure 7F–G, S7C). LPS supplementation also partially improved GI transit time (Figure 7H) and reduced cecum size (Figure S7G).

Next, we asked whether the MM-neuronal crosstalk is reversible. Antibiotic-treated mice were reconstituted with microbiota following fecal transfer (FT) from untreated control mice. Repopulation of luminal bacteria to nearly normal levels (Figure S7H) was able to restore *Csf1* expression (Figure 7F) and MM numbers (Figure 7G) in the gut and correct dysmotility (Figure 7I) and cecum size (Figure S7I).

Taken together, these results demonstrate that the function of both components of macrophage-neuronal crosstalk can be reversibly modified by luminal commensals.

DISCUSSION

MMs are thought to regulate GI motility during inflammation through secretion of inflammatory cytokines and the recruitment of inflammatory cells, which further accelerate the inflammatory process (Boeckxstaens and de Jonge, 2009; Mikkelsen, 2010; Wehner et al., 2007). This mechanism, however, has not been proven directly to occur. Our data demonstrate that MMs regulate GI motility even when the bowel is not inflamed and MMs do so through production of the soluble growth factor, BMP2. Whether BMP2 remains a key factor in regulating GI motility during inflammation remains to be determined.

Our study suggests that MM-derived BMP2 regulates functional activity of neurons that transcends the known role of this growth factor in neuronal development (Chalazonitis et al., 2004; Chalazonitis et al., 2008). While MMs or MM-specific BMP2 may contribute to ENS development as suggested by our data from $Csf1^{op/op}$ mice, the mechanisms by which BMPs affect homeostasis or function(s) of differentiated enteric neurons are not clear. Studies of BMPR signaling in motoneurons at the neuromuscular junction of developing *Drosophila* larvae suggest that BMPR signaling regulates: (i) microtubule stability of axons, (ii) fast axonal transport, (iii) synaptic growth and stability (Aberle et al., 2002; Eaton and Davis,

2005; Eaton et al., 2002; Nahm et al., 2013; Wang et al., 2007). More recently, BMPs have been demonstrated to inhibit constitutive electrical activity in differentiating neurons of the developing *Xenopus* spinal cord (Swapna and Borodinsky, 2012). We postulate that BMPs may exert similar effects on adult neurons. It is also possible that additional MM derived factors can affect the function of enteric neurons. A recent study revealed the role of the resident macrophages of the CNS, the microglia, in promoting learning dependent synapse formation by providing brain-derived neurotrophic factor (BDNF) to neurons (Parkhurst et al., 2013). Likewise, macrophage populations at other sites may participate in regulating the physiology of organs through mechanisms similar to those observed in the gut and the brain.

Reduction of BMP2 expression in mice after antibiotic treatment implies that MMs are sensitive to changes in the luminal environment, but the mechanism of this sensing remains unknown. Interestingly, prolonged *Helicobacter hepaticus* infection has been shown to dramatically affect MM activation and behavior even though *Helicobacter* never crosses the epithelial barrier of the gut (Hoffman and Fleming, 2010). It appears plausible that alterations of MMs occur through a combination of downstream immune and neuronal surveillance in the mucosa including signals provided by Toll-like receptor positive enteroendocrine cells (Bogunovic et al., 2007). It is also possible that MMs recognize commensal components directly by sensing systemic LPS found in the serum of normal mice (Anitha et al., 2012; Uramatsu et al., 2010).

Chronic disruption of normal peristaltic activity is a characteristic symptom of functional gastrointestinal disorders such as irritable bowel syndrome (IBS). In IBS patients, dysmotility-related symptoms are often accompanied by symptoms associated with visceral hypersensitivity, an exaggerated perceptual response to peripheral stimuli that could result from altered processing of visceral neuronal afferent signals (Faure et al., 2007a). Histological analysis of full-thickness intestinal biopsies from IBS patients revealed signs of degenerative or inflammatory neuropathy (Lindberg et al., 2009; Tornblom et al., 2002). Changes in the microbial environment, such as a preceding bacterial GI infection and small bowel bacterial overgrowth, have been proposed to be causes of IBS (Peralta et al., 2009; Pimentel et al., 2000, 2003; Pimentel et al., 2002). An improved understanding of the interplay between enteric neurons, MMs and luminal signals may thus provide new therapeutic strategies for the treatment and/or prevention of IBS.

EXPERIMENTAL PROCEDURES

Mice

All mice were housed in a specific pathogen-free environment at Mount Sinai School of Medicine and Penn State College of Medicine and were used in accordance with protocols approved by the Institutional Animal Care and Utilization Committees. The list of mouse strains is provided in the Extended Experimental Procedures.

MP depletion was achieved by single i.p. injection of 37.5 μg/mg αCSF1R mAb [clone AFS98 (Sudo et al., 1995)] purified from hybridomas as described (Hashimoto et al., 2011a).

Cell isolation, flow cytometry and cell sorting

Single cells suspensions of intestinal muscularis externa or entire bowel were prepared, analyzed and purified as described (Bogunovic et al., 2009).

Immunofluorescence

Separated intestinal muscularis externa or cultured enteric neurons were stained following the described protocol (Bogunovic et al., 2009) with some modifications and using commercial reagents described in the Supplemental Experimental Procedures.

Whole mouse genome microarray was performed and normalized by Immgen Project (www.immgen.org) as described (Miller et al., 2012).

Real-time PCR was performed as described (Bogunovic et al., 2009) with some modifications explained in the Extended Experimental Procedures. The data were normalized to β-actin. Each data dot on sorted primary cells is obtained by analyzing RNA from 50,000 cells purified from 5–7 mice. Each data dot from cultured neurons is obtained by analyzing RNA from an independent primary neuronal culture.

Colonic peristalsis *ex vivo*

The technique is described in the Extended Experimental Procedures. To block BMPR signaling 13mg/g (Helbing et al., 2011) of dorsomorphin (Sigma) in DMSO was injected i.p. 18 and 2 hours prior to analysis. In BMP2 “rescue” experiments the colonic rings were distended until 2.75 mm. A baseline recording of 40 minutes was taken, after which recombinant human BMP2 (R&D Systems) dissolved in 4 mM HCl was cumulatively added to the bath (1, 5, 10 ng per 8mL organ bath) followed by 10 minutes of recording between doses. Dose response to KCl was performed by distending colonic rings until a baseline force of 0.5 mN was achieved. The rings were allowed to equilibrate for 2.5 hours, with hourly solution changes. Increasing concentrations of KCl (0, 10, 40, 80, 100, and 200 mM) were added to the bath and solution was changed after 5 minutes. Ratios were calculated as baseline force prior to KCl addition over maximal contractile force after.

Gastrointestinal motility

Colonic transit time was detected by bead expulsion assay (Li et al., 2006); gastric emptying, small bowel transit and total intestinal transit time were measured as described (Li et al., 2011). Control and experimental groups were age and sex matched. For *in vivo* “rescue” experiment human recombinant BMP2 (Peprotech) was injected i.p. (50 ng/g of body weight) 18 and 3 hrs prior measuring colonic transit time.

Epithelial permeability studies were performed as described (Dahan et al., 2011).

***In vitro* culture of enteric neurons** was prepared from embryonic intestines from E17 as described in the Extended Experimental Procedures.

Antibiotic treatment

A variation of a published protocol (Rakoff-Nahoum et al., 2004) was used. Six-seven week old female mice were given drinking water containing 1g/l of ampicillin (Teknova), 1g/l of streptomycin (Gibco), 1 g/l of metronidazole (Sigma) and 1 g/l of vancomycin (Sigma) for 1–4 weeks. For LPS supplementation mice were given 50 μg/ml of LPS from E.coli O111:B4 (Sigma) in drinking water (Rakoff-Nahoum et al., 2004) together with antibiotics for 4 weeks.

Fecal transfer

Recipient mice were placed on antibiotic-free water 24 hours prior fecal transfer. Intestinal contents from donor mice prepared as described in the Extended Experimental Procedures were given to recipient mice by oral gavage. Donor mice were age-matched, obtained from the same vendor and maintained in the same facility as the recipients of fecal transfer.

Bacterial 16S rDNA qPCR to quantify fecal bacterial DNA was performed as described in the Extended Experimental Procedures.

Statistical analysis

Data are presented as mean ± SEM. The statistical significance of differences between group means was determined with the two-tailed unpaired or paired Student's t test and one-way ANOVA. Values of $P< 0.05$ (*), $P<0.005$ (**) and $P<0,0005$ (***) indicate statistical significance.

Supplementary Material

Refer to Web version on PubMed Central for supplementary material.

Acknowledgments

We would like to thank Immgen Project (http://www.immgen.org) for performing a whole mouse genome microarray. We would like to thank Frederico Costa Pinta (Rockefeller University, New York, NY, and School of Veterinary Medicine, University of Sao Paulo, Brazil), Hongyan Zou (Mount Sinai School of Medicine, New York, NY) and Florent Ginhoux (Singapore Immunology Network and Agency for Science, Technology and Research, Singapore) for productive discussions regarding the study and Aron Lukacher (Penn State University College of Medicine, Hershey, PA) for help with the manuscript. This work is in part supported by NIH AI09561, CA173861 and AI104848 (M.M.), CA32551 (E.R.S), R21-AI105047 (D.M.) as well as CDA from CCFA and PCARS from NIAID (M.B.).

REFERENCES

Aberle H, Haghighi AP, Fetter RD, McCabe BD, Magalhaes TR, Goodman CS. wishful thinking encodes a BMP type II receptor that regulates synaptic growth in Drosophila. Neuron. 2002; 33:545–558. [PubMed: 11856529]

Abrams GD, Bishop JE. Effect of the normal microbial flora on gastrointestinal motility. Proc Soc Exp Biol Med. 1967; 126:301–304. [PubMed: 6066182]

Anderson L, Lowery JW, Frank DB, Novitskaya T, Jones M, Mortlock DP, Chandler RL, de Caestecker MP. Bmp2 and Bmp4 exert opposing effects in hypoxic pulmonary hypertension. American journal of physiology Regulatory, integrative and comparative physiology. 2010; 298:R833–R842.

Anitha M, Vijay-Kumar M, Sitaraman SV, Gewirtz AT, Srinivasan S. Gut microbial products regulate murine gastrointestinal motility via Toll-like receptor 4 signaling. Gastroenterology. 2012; 143:1006–1016. e1004. [PubMed: 22732731]

Boeckxstaens GE, de Jonge WJ. Neuroimmune mechanisms in postoperative ileus. Gut. 2009; 58:1300–1311. [PubMed: 19671558]

Bogunovic M, Dave SH, Tilstra JS, Chang DT, Harpaz N, Xiong H, Mayer LF, Plevy SE. Enteroendocrine cells express functional Toll-like receptors. Am J Physiol Gastrointest Liver Physiol. 2007; 292:G1770–G1783. [PubMed: 17395901]

Bogunovic M, Ginhoux F, Helft J, Shang L, Hashimoto D, Greter M, Liu K, Jakubzick C, Ingersoll MA, Leboeuf M, et al. Origin of the lamina propria dendritic cell network. Immunity. 2009; 31:513–525. [PubMed: 19733489]

Bogunovic M, Mortha A, Muller PA, Merad M. Mononuclear phagocyte diversity in the intestine. Immunologic research. 2012; 54:37–49. [PubMed: 22562804]

Bulbring E, Crema A. The action of 5-hydroxytryptamine, 5-hydroxytryptophan and reserpine on intestinal peristalsis in anaesthetized guineapigs. J Physiol. 1959a; 146:29–53. [PubMed: 13655214]

Bulbring E, Crema A. The release of 5-hydroxytryptamine in relation to pressure exerted on the intestinal mucosa. J Physiol. 1959b; 146:18–28. [PubMed: 13655213]

Chalazonitis A, D'Autreaux F, Guha U, Pham TD, Faure C, Chen JJ, Roman D, Kan L, Rothman TP, Kessler JA, et al. Bone morphogenetic protein-2 and −4 limit the number of enteric neurons but promote development of a TrkC-expressing neurotrophin-3-dependent subset. J Neurosci. 2004; 24:4266–4282. [PubMed: 15115823]

Chalazonitis A, D'Autreaux F, Pham TD, Kessler JA, Gershon MD. Bone morphogenetic proteins regulate enteric gliogenesis by modulating ErbB3 signaling. Dev Biol. 2011; 350:64–79. [PubMed: 21094638]

Chalazonitis A, Pham TD, Li Z, Roman D, Guha U, Gomes W, Kan L, Kessler JA, Gershon MD. Bone morphogenetic protein regulation of enteric neuronal phenotypic diversity: relationship to timing of cell cycle exit. J Comp Neurol. 2008; 509:474–492. [PubMed: 18537141]

Chow A, Huggins M, Ahmed J, Hashimoto D, Lucas D, Kunisaki Y, Pinho S, Leboeuf M, Noizat C, van Rooijen N, et al. CD169(+) macrophages provide a niche promoting erythropoiesis under homeostasis and stress. Nature medicine. 2013; 19:429–436.

Chow A, Lucas D, Hidalgo A, Mendez-Ferrer S, Hashimoto D, Scheiermann C, Battista M, Leboeuf M, Prophete C, van Rooijen N, et al. Bone marrow CD169+ macrophages promote the retention of hematopoietic stem and progenitor cells in the mesenchymal stem cell niche. The Journal of experimental medicine. 2011; 208:261–271. [PubMed: 21282381]

Dahan S, Rabinowitz KM, Martin AP, Berin MC, Unkeless JC, Mayer L. Notch-1 signaling regulates intestinal epithelial barrier function, through interaction with CD4+ T cells, in mice and humans. Gastroenterology. 2011; 140:550–559. [PubMed: 21056041]

Derynck R, Zhang YE. Smad-dependent and Smad-independent pathways in TGF-beta family signalling. Nature. 2003; 425:577–584. [PubMed: 14534577]

Eaton BA, Davis GW. LIM Kinase1 controls synaptic stability downstream of the type II BMP receptor. Neuron. 2005; 47:695–708. [PubMed: 16129399]

Eaton BA, Fetter RD, Davis GW. Dynactin is necessary for synapse stabilization. Neuron. 2002; 34:729–741. [PubMed: 12062020]

Faure C, Bouin M, Poitras P. Visceral hypersensitivity in irritable bowel syndrome: does it really normalize over time? Gastroenterology. 2007a; 132:464–465. author reply 465. [PubMed: 17241900]

Faure C, Chalazonitis A, Rheaume C, Bouchard G, Sampathkumar SG, Yarema KJ, Gershon MD. Gangliogenesis in the enteric nervous system: roles of the polysialylation of the neural cell adhesion molecule and its regulation by bone morphogenetic protein-4. Dev Dyn. 2007b; 236:44–59. [PubMed: 16958105]

Flores-Langarica A, Meza-Perez S, Calderon-Amador J, Estrada-Garcia T, Macpherson G, Lebecque S, Saeland S, Steinman RM, Flores-Romo L. Network of dendritic cells within the muscular layer of the mouse intestine. Proceedings of the National Academy of Sciences of the United States of America. 2005; 102:19039–19044. [PubMed: 16361439]

Frigo GM, Lecchini S. An improved method for studying the peristaltic reflex in the isolated colon. British journal of pharmacology. 1970; 39:346–356. [PubMed: 5425278]

Fu M, Vohra BP, Wind D, Heuckeroth RO. BMP signaling regulates murine enteric nervous system precursor migration, neurite fasciculation, and patterning via altered Ncam1 polysialic acid addition. Dev Biol. 2006; 299:137–150. [PubMed: 16952347]

Furness JB. The enteric nervous system and neurogastroenterology. Nature reviews Gastroenterology & hepatology. 2012; 9:286–294.

Goldstein AM, Brewer KC, Doyle AM, Nagy N, Roberts DJ. BMP signaling is necessary for neural crest cell migration and ganglion formation in the enteric nervous system. Mech Dev. 2005; 122:821–833. [PubMed: 15905074]

Greter M, Lelios I, Pelczar P, Hoeffel G, Price J, Leboeuf M, Kundig TM, Frei K, Ginhoux F, Merad M, et al. Stroma-derived interleukin-34 controls the development and maintenance of langerhans cells and the maintenance of microglia. Immunity. 2012; 37:1050–1060. [PubMed: 23177320]

Gustafsson BE, Midtvedt T, Strandberg K. Effects of microbial contamination on the cecum enlargement of germfree rats. Scandinavian journal of gastroenterology. 1970; 5:309–314. [PubMed: 5429896]

Hashimoto D, Chow A, Greter M, Saenger Y, Kwan WH, Leboeuf M, Ginhoux F, Ochando JC, Kunisaki Y, van Rooijen N, et al. Pretransplant CSF-1 therapy expands recipient macrophages and ameliorates GVHD after allogeneic hematopoietic cell transplantation. The Journal of experimental medicine. 2011a; 208:1069–1082. [PubMed: 21536742]

Hashimoto D, Miller J, Merad M. Dendritic cell and macrophage heterogeneity in vivo. Immunity. 2011b; 35:323–335. [PubMed: 21943488]

Helbing T, Rothweiler R, Ketterer E, Goetz L, Heinke J, Grundmann S, Duerschmied D, Patterson C, Bode C, Moser M. BMP activity controlled by BMPER regulates the proinflammatory phenotype of endothelium. Blood. 2011; 118:5040–5049. [PubMed: 21900199]

Heredia DJ, Gershon MD, Koh SD, Corrigan RD, Okamoto T, Smith TK. Important role of mucosal serotonin in colonic propulsion and peristaltic reflexes: in vitro analyses in mice lacking tryptophan hydroxylase 1. J Physiol. 2013; 591:5939–5957. [PubMed: 24127620]

Hoffman SM, Fleming SD. Natural Helicobacter infection modulates mouse intestinal muscularis macrophage responses. Cell Biochem Funct. 2010; 28:686–694. [PubMed: 21104937]

Hogan BL. Bone morphogenetic proteins: multifunctional regulators of vertebrate development. Genes & development. 1996; 10:1580–1594. [PubMed: 8682290]

Huizinga JD, Thuneberg L, Kluppel M, Malysz J, Mikkelsen HB, Bernstein A. W/kit gene required for interstitial cells of Cajal and for intestinal pacemaker activity. Nature. 1995; 373:347–349. [PubMed: 7530333]

Huynh D, Dai XM, Nandi S, Lightowler S, Trivett M, Chan CK, Bertoncello I, Ramsay RG, Stanley ER. Colony stimulating factor-1 dependence of paneth cell development in the mouse small intestine. Gastroenterology. 2009; 137:136–144. 144 e131-133. [PubMed: 19303020]

Kirsch T, Nickel J, Sebald W. BMP-2 antagonists emerge from alterations in the low-affinity binding epitope for receptor BMPR-II. The EMBO journal. 2000; 19:3314–3324. [PubMed: 10880444]

Li Z, Chalazonitis A, Huang YY, Mann JJ, Margolis KG, Yang QM, Kim DO, Cote F, Mallet J, Gershon MD. Essential roles of enteric neuronal serotonin in gastrointestinal motility and the development/survival of enteric dopaminergic neurons. The Journal of neuroscience : the official journal of the Society for Neuroscience. 2011; 31:8998–9009. [PubMed: 21677183]

Li ZS, Schmauss C, Cuenca A, Ratcliffe E, Gershon MD. Physiological modulation of intestinal motility by enteric dopaminergic neurons and the D2 receptor: analysis of dopamine receptor expression, location, development, and function in wild-type and knock-out mice. The Journal of neuroscience : the official journal of the Society for Neuroscience. 2006; 26:2798–2807. [PubMed: 16525059]

Lin H, Lee E, Hestir K, Leo C, Huang M, Bosch E, Halenbeck R, Wu G, Zhou A, Behrens D, et al. Discovery of a cytokine and its receptor by functional screening of the extracellular proteome. Science. 2008; 320:807–811. [PubMed: 18467591]

Lindberg G, Tornblom H, Iwarzon M, Nyberg B, Martin JE, Veress B. Full-thickness biopsy findings in chronic intestinal pseudo-obstruction and enteric dysmotility. Gut. 2009; 58:1084–1090. [PubMed: 19136514]

Mikkelsen HB. Interstitial cells of Cajal, macrophages and mast cells in the gut musculature: morphology, distribution, spatial and possible functional interactions. Journal of cellular and molecular medicine. 2010; 14:818–832. [PubMed: 20132411]

Mikkelsen HB, Rumessen JJ. Characterization of macrophage-like cells in the external layers of human small and large intestine. Cell and tissue research. 1992; 270:273–279. [PubMed: 1451172]

Mikkelsen HB, Thuneberg L. Op/op mice defective in production of functional colony-stimulating factor-1 lack macrophages in muscularis externa of the small intestine. Cell and tissue research. 1999; 295:485–493. [PubMed: 10022968]

Mikkelsen HB, Thuneberg L, Rumessen JJ, Thorball N. Macrophage-like cells in the muscularis externa of mouse small intestine. The Anatomical record. 1985; 213:77–86. [PubMed: 2416252]

Miller JC, Brown BD, Shay T, Gautier EL, Jojic V, Cohain A, Pandey G, Leboeuf M, Elpek KG, Helft J, et al. Deciphering the transcriptional network of the dendritic cell lineage. Nat Immunol. 2012; 13:888–899. [PubMed: 22797772]

Nahm M, Lee MJ, Parkinson W, Lee M, Kim H, Kim YJ, Kim S, Cho YS, Min BM, Bae YC, et al. Spartin regulates synaptic growth and neuronal survival by inhibiting BMP-mediated microtubule stabilization. Neuron. 2013; 77:680–695. [PubMed: 23439121]

Nandi S, Gokhan S, Dai XM, Wei S, Enikolopov G, Lin H, Mehler MF, Stanley ER. The CSF-1 receptor ligands IL-34 and CSF-1 exhibit distinct developmental brain expression patterns and regulate neural progenitor cell maintenance and maturation. Dev Biol. 2012; 367:100–113. [PubMed: 22542597]

Parkhurst CN, Yang G, Ninan I, Savas JN, Yates JR, Lafaille JJ 3rd, Hempstead BL, Littman DR, Gan WB. Microglia promote learning-dependent synapse formation through brain-derived neurotrophic factor. Cell. 2013; 155:1596–1609. [PubMed: 24360280]

Peralta S, Cottone C, Doveri T, Almasio PL, Craxi A. Small intestine bacterial overgrowth and irritable bowel syndrome-related symptoms: experience with Rifaximin. World journal of gastroenterology : WJG. 2009; 15:2628–2631. [PubMed: 19496193]

Pimentel M, Chow EJ, Lin HC. Eradication of small intestinal bacterial overgrowth reduces symptoms of irritable bowel syndrome. The American journal of gastroenterology. 2000; 95:3503–3506. [PubMed: 11151884]

Pimentel M, Chow EJ, Lin HC. Normalization of lactulose breath testing correlates with symptom improvement in irritable bowel syndrome. a double-blind, randomized, placebo-controlled study. The American journal of gastroenterology. 2003; 98:412–419. [PubMed: 12591062]

Pimentel M, Soffer EE, Chow EJ, Kong Y, Lin HC. Lower frequency of MMC is found in IBS subjects with abnormal lactulose breath test, suggesting bacterial overgrowth. Digestive diseases and sciences. 2002; 47:2639–2643. [PubMed: 12498278]

Rakoff-Nahoum S, Paglino J, Eslami-Varzaneh F, Edberg S, Medzhitov R. Recognition of commensal microflora by toll-like receptors is required for intestinal homeostasis. Cell. 2004; 118:229–241. [PubMed: 15260992]

Reigstad CS, Kashyap PC. Beyond phylotyping: understanding the impact of gut microbiota on host biology. Neurogastroenterology and motility : the official journal of the European Gastrointestinal Motility Society. 2013; 25:358–372. [PubMed: 23594242]

Rumessen JJ, Vanderwinden JM. Interstitial cells in the musculature of the gastrointestinal tract: Cajal and beyond. International review of cytology. 2003; 229:115–208. [PubMed: 14669956]

Sudo T, Nishikawa S, Ogawa M, Kataoka H, Ohno N, Izawa A, Hayashi S, Nishikawa S. Functional hierarchy of c-kit and c-fms in intramarrow production of CFU-M. Oncogene. 1995; 11:2469–2476. [PubMed: 8545103]

Swapna I, Borodinsky LN. Interplay between electrical activity and bone morphogenetic protein signaling regulates spinal neuron differentiation. Proceedings of the National Academy of Sciences of the United States of America. 2012; 109:16336–16341. [PubMed: 22991474]

Tornblom H, Lindberg G, Nyberg B, Veress B. Full-thickness biopsy of the jejunum reveals inflammation and enteric neuropathy in irritable bowel syndrome. Gastroenterology. 2002; 123:1972–1979. [PubMed: 12454854]

Uramatsu M, Matsumoto T, Tateda K, Shibuya K, Miyazaki S, Horino T, Tanabe M, Sumiyama Y, Kusachi S, Yamaguchi K. Involvement of endotoxin in the mortality of mice with gut-derived sepsis due to methicillin-resistant Staphylococcus aureus. Microbiology and immunology. 2010; 54:330–337. [PubMed: 20536731]

Wang X, Shaw WR, Tsang HT, Reid E, O'Kane CJ. Drosophila spichthyin inhibits BMP signaling and regulates synaptic growth and axonal microtubules. Nature neuroscience. 2007; 10:177–185.

Wang Y, Szretter KJ, Vermi W, Gilfillan S, Rossini C, Cella M, Barrow AD, Diamond MS, Colonna M. IL-34 is a tissue-restricted ligand of CSF1R required for the development of Langerhans cells and microglia. Nat Immunol. 2012; 13:753–760. [PubMed: 22729249]

Wehner S, Behrendt FF, Lyutenski BN, Lysson M, Bauer AJ, Hirner A, Kalff JC. Inhibition of macrophage function prevents intestinal inflammation and postoperative ileus in rodents. Gut. 2007; 56:176–185. [PubMed: 16809419]

Wiktor-Jedrzejczak W, Urbanowska E, Aukerman SL, Pollard JW, Stanley ER, Ralph P, Ansari AA, Sell KW, Szperl M. Correction by CSF-1 of defects in the osteopetrotic op/op mouse suggests local, developmental, and humoral requirements for this growth factor. Exp Hematol. 1991; 19:1049–1054. [PubMed: 1915705]

Wynn TA, Chawla A, Pollard JW. Macrophage biology in development, homeostasis and disease. Nature. 2013; 496:445–455. [PubMed: 23619691]

Yeung YG, Jubinsky PT, Sengupta A, Yeung DC, Stanley ER. Purification of the colony-stimulating factor 1 receptor and demonstration of its tyrosine kinase activity. Proc Natl Acad Sci U S A. 1987; 84:1268–1271. [PubMed: 3029775]

Yu PB, Hong CC, Sachidanandan C, Babitt JL, Deng DY, Hoyng SA, Lin HY, Bloch KD, Peterson RT. Dorsomorphin inhibits BMP signals required for embryogenesis and iron metabolism. Nature chemical biology. 2008; 4:33–41.

Zhang H, Bradley A. Mice deficient for BMP2 are nonviable and have defects in amnion/chorion and cardiac development. Development. 1996; 122:2977–2986. [PubMed: 8898212]

HIGHLIGHTS

- Muscularis macrophages produce BMP2 that activates BMPR on enteric neurons
- Enteric neurons produce CSF1 that promotes homeostasis of muscularis macrophages
- Macrophage-neuronal crosstalk regulates constitutive gastrointestinal motility
- Macrophage-neuronal crosstalk is driven by gut microbiota

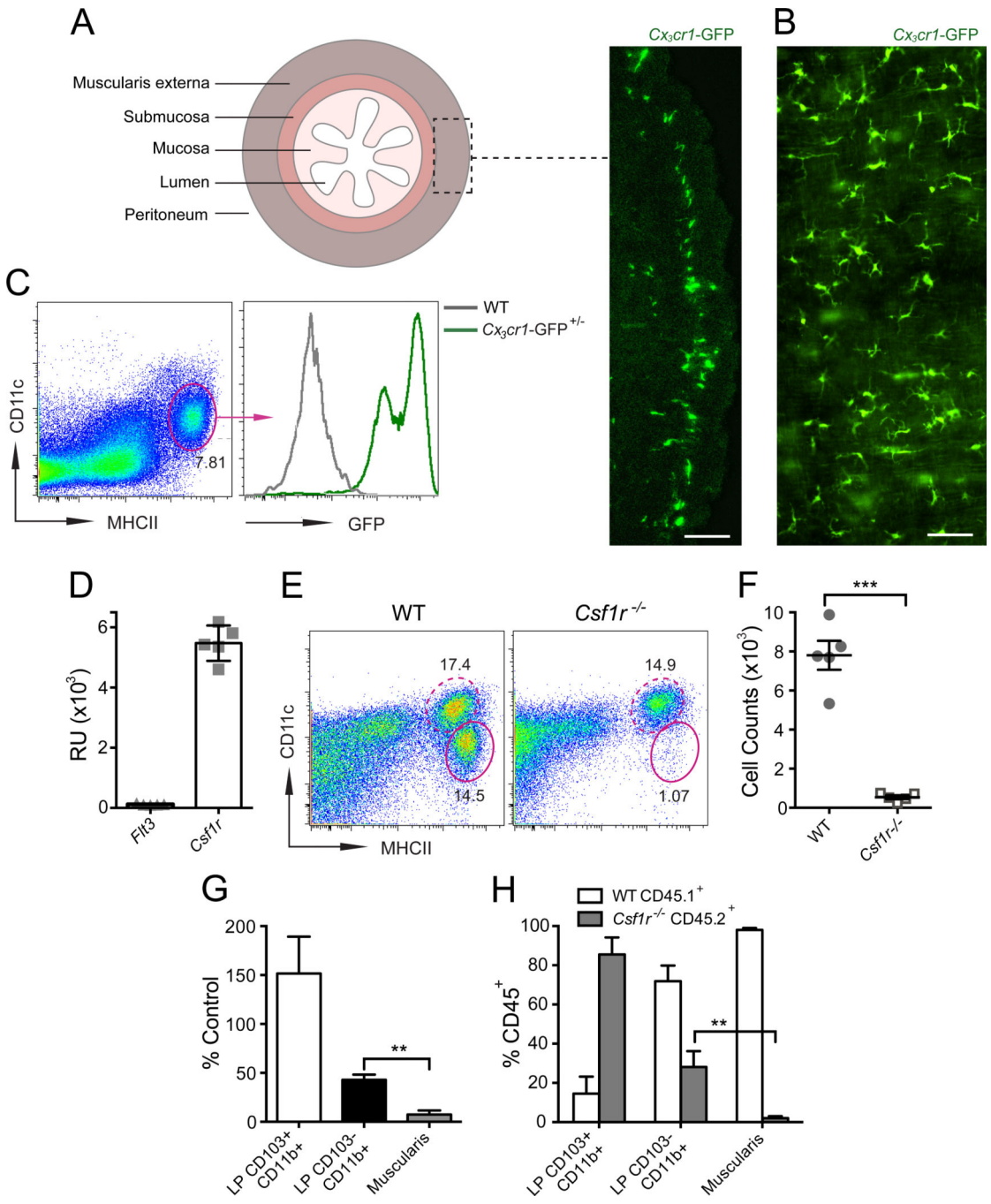

Figure 1. MHCII^{+}CX$_3$CR1^{+} MMs require CSF1R signaling for their development

(A–B) Distribution of CX$_3$CR1^{+} MMs shown in cross-section (A) or muscularis sheet (B) of large bowel (LB) from *Cx$_3$cr1*-GFP$^{+/–}$ mice. Scale bar – 100 nm. (C) Phenotype of MMs in small bowel (SB) muscularis from *Cx$_3$cr1*-GFP$^{+/–}$ mice by FACS analysis (gated on DAPI$^{–}$ cells). (D) *Flt3* and *Csf1r* gene expression in sorted MMs measured by whole mouse genome microarray and presented as relative units (RU). (E) FACS plots of whole bowel suspensions from WT or *Cscf1r*$^{–/–}$ mice show % of CD11c^{lo}MHCII^{hi} MMs (oval gate, solid line) and CD11c^{hi}MHCII^{hi} LP phagocytes (oval gate, dashed line). Gated on

$CD45^+CD11c^{lo/hi}CD11b^{lo/hi}$ cells as demonstrated in Figure S1. (F) Absolute numbers of MMs in total gut of WT and *Csf1r*$^{-/-}$ mice quantified by FACS. (G) Relative reduction of MMs and $CD103^+CD11b^+$ and $CD103^-CD11b^+$ LP phagocytes in *Csf1r*$^{-/-}$ mice as compared to WT littermates (quantified by FACS). (H) % of WT $CD45.1^+$ and *Csf1r*$^{-/-}$ $CD45.2^+$ cells among $CD45^+$ LP $CD103^+CD11b^+$ and LP $CD103^-CD11b^+$ phagocytes and MMs (Muscularis) in SB from 10% WT + 90% *Csf1r*$^{-/-}$ mixed BM chimeras.

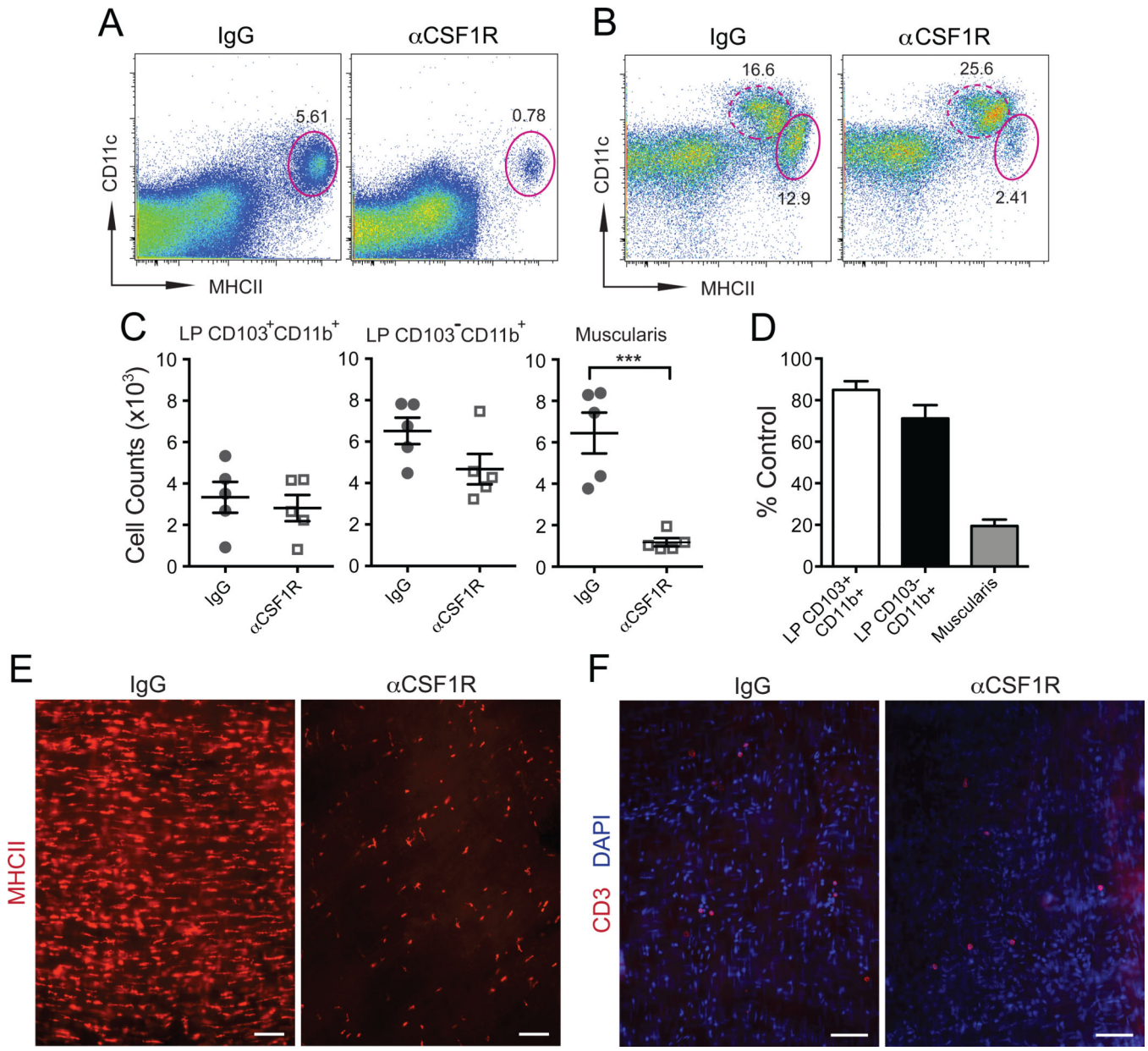

Figure 2. Model of MM depletion

(A–B) FACS plots of separated SB muscularis (A) and whole SB (B) single cell suspensions from WT mice 2 days after i.p. injection of isotype IgG or αCSF1R mAb show % of $CD11c^{lo}MHCII^{hi}$ MMs (oval gate, solid line) and $CD11c^{hi}MHCII^{hi}$ LP phagocytes (oval gate, dashed line). A – gated on total viable cells. B – gated on $CD45^{+}CD11c^{lo/hi}CD11b^{lo/hi}$ cells using the gating strategy as in Figure S1. (C) Absolute numbers of LP $CD103^{+}CD11b^{+}$ and LP $CD103^{-}CD11b^{+}$ phagocyte and MMs (Muscularis) in SB of WT mice 2 days after i.p. injection with isotype IgG or αCSF1R mAb quantified by FACS. (D) Relative reduction of LP phagocyte and MM numbers quantified by FACS in WT mice treated with αCSF1R mAb (Day 2) as compared to isotype IgG treated mice. (E–F) Distribution of $MHCII^{+}$ macrophages (E) and $CD3^{+}$ T cells (F) in LB muscularis from WT mice 2 days after i.p.

injection of isotype IgG or αCSF1R mAb analyzed by immunofluorescence (IF). Scale bars – 100 nm.

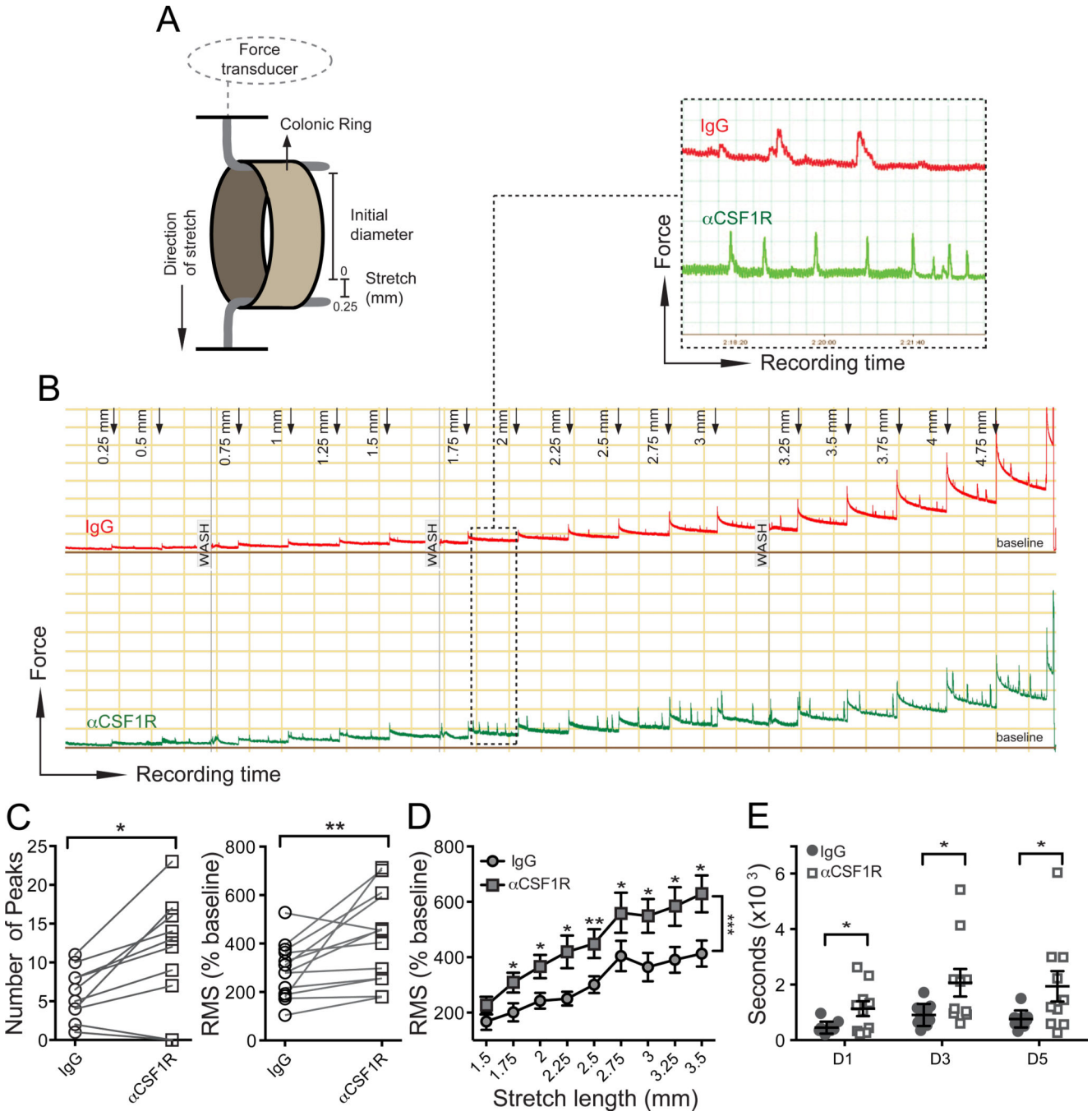

Figure 3. Depletion of MMs results in intestinal dysmotility

(A) Illustration of *ex vivo* method to measure stretch-induced peristaltic contractions of colonic rings using a myograph. (B) Five hour recording of stretch-induced contractions of colonic rings during repeated application of 0.25 mm long stretching up to 5.00 mm total stretch length. 3 mm colonic rings were obtained from WT mice 2 days after i.p. injection of isotype IgG or αCSF1R mAb. (C) Number of peaks (left) or Root Mean Square (RMS) normalized to baseline in % (right) during 10 min recordings of colonic contraction at stretch distance 2.75 mm. (D) RMS normalized to baseline (%) during 10 min recordings of

colonic contractions at each stretching step from 1.5 to 3.5 mm. (E) Colonic transit time measured by bead expulsion assay in WT mice 1, 3 and 5 days after i.p. injection of isotype IgG or αCSF1R mAb.

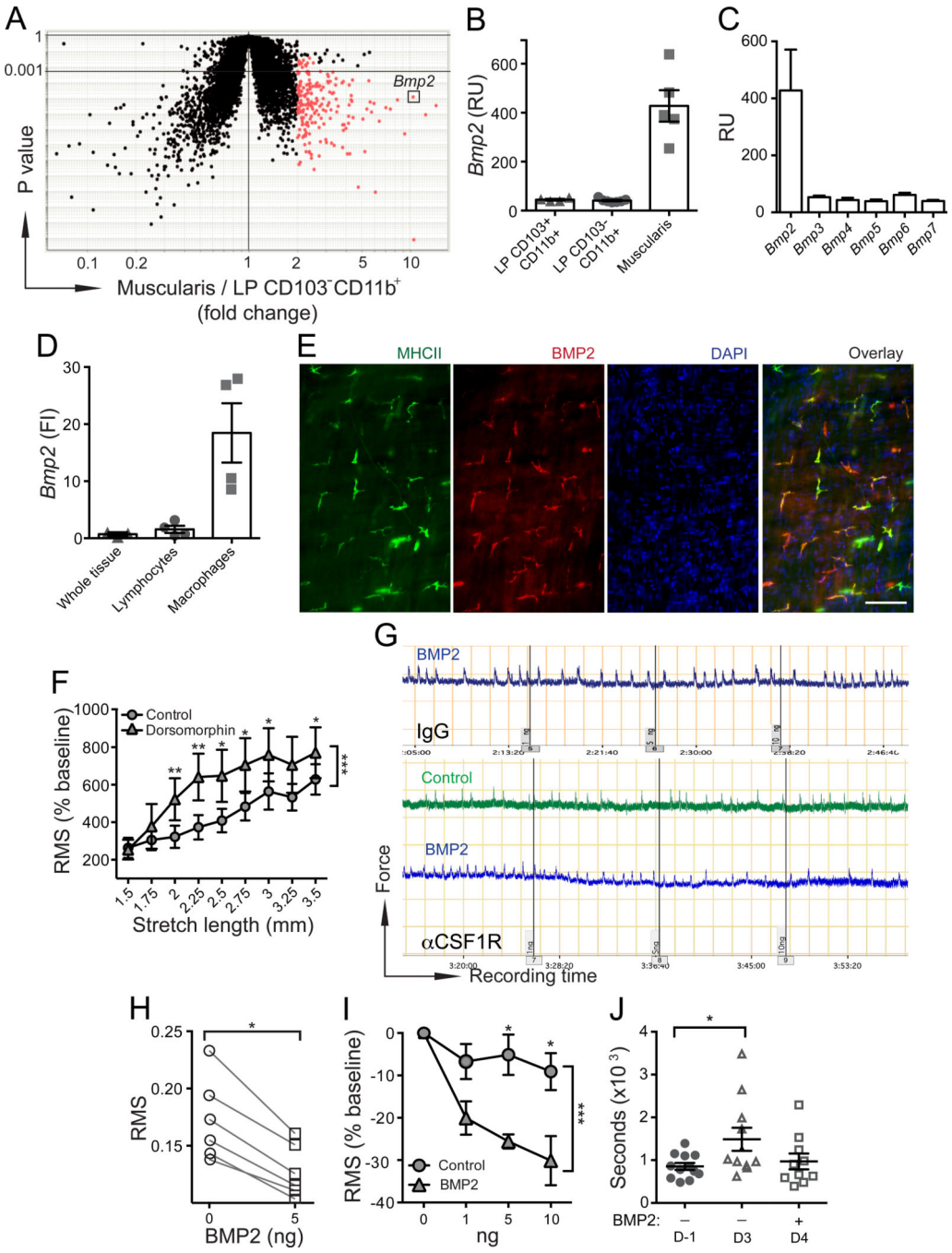

Figure 4. MMs regulate intestinal peristalsis by secreting BMP2

(A–B) *Bmp2* gene expression levels in MMs (Muscularis) compared to LP CD103^{-}CD11b^{+} phagocytes (A) and LP CD103^{+}CD11b^{+} and LP CD103^{-}CD11b^{+} phagocytes (B) measured by whole mouse genome microarray. (C) *Bmp2-7* gene expression levels in MMs measured by whole mouse genome microarray. (D) *Bmp2* relative gene expression levels measured by qPCR in intact SB muscularis (whole tissue) or in SSC^{lo}CD45^{+}CD11b^{-} lymphocytes and macrophages sorted from separated SB muscularis. FI – fold increase as compared to "whole tissue". (E) IF analysis of LB muscularis from WT mice stained with anti-BMP2 and

anti-MHCII mAbs and counterstained with DAPI. Scale bar – 100 nm. (F) RMS of colonic contraction recordings normalized to baseline (%) at stretch intervals 1.5–3.5 mm. 3 mm colonic rings were obtained from WT mice treated with BMP receptor inhibitor dorsomorphin or control vehicle. (G) WT mice were injected i.p. with isotype IgG (top) or αCSF1R mAb (bottom) and analyzed 2 days later. Panels show *ex vivo* recordings of stretch-induced contractions of colonic rings from these mice before and after adding 1, 5 and 10 ng of human recombinant BMP2 or control vehicle (performed at 2.75 mm "optimal" stretch distance). (H) RMS of 10 min recordings described in F (bottom panel, αCSF1R mAb treated mice) before and after adding 5 ng of BMP2. (I) RMS normalized to baseline (%) of recordings described in F (bottom panel, αCSF1R mAb treated mice) after adding BMP2 (1, 5, 10 ng) or control vehicle. Baseline here is the recording at the same stretch distance (2.75 mm) prior to adding BMP2 or control vehicle. (J) Colonic transit time measured by bead expulsion assay in WT mice prior receiving αCSF1R mAb (day −1) and on days 3 and 4 after receiving αCSF1R mAb; 18 and 3 hours prior the last assessment (day 4) mice received 1 μg of BMP2 i.p.

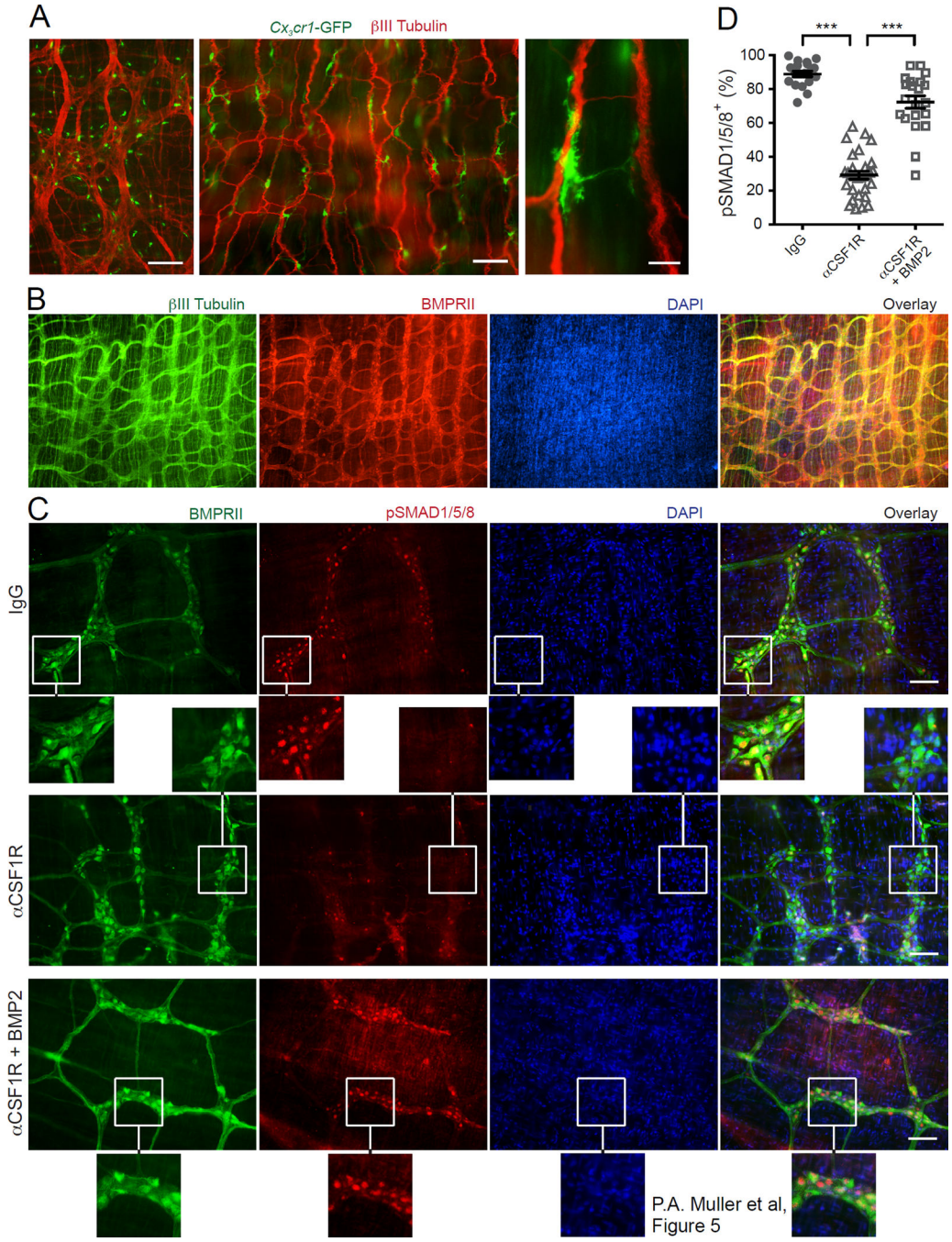

Figure 5. MMs activate BMP2 receptor on enteric neurons

(A) Distribution of CX_3CR1^+ MMs in colon (left) and ileum (middle and right) muscularis from *Cx3cr1*-$GFP^{+/-}$ mice stained with anti- βIII Tubulin Ab and analyzed by IF. Scale bars – 500 nm (left), 100 nm (middle) and 10 nm (right). (B) IF analysis of LB muscularis from WT mice stained with anti-BMPRII and anti-βIII Tubulin Abs and counterstained with DAPI. Scale bars – 500 nm. (C) IF analysis of LB muscularis from WT mice 2 days after i.p. injection of isotype IgG (top), αCSF1R mAb (middle and bottom) stained with anti-pSMAD1/5/8 and anti-BMPRII Abs and counterstained with DAPI. The bottom panel

shows pSMAD1/5/8 distribution in the muscularis from αCSF1R mAb injected mouse that was incubated with BMP2 as described in D. Scale bars – 100 nm. (D) Quantitative summary of the distribution of pSMAD1/5/8^{+}BMPRII^{+} neurons in the muscularis from WT mice 2 days after i.p. injection of isotype IgG or αCSF1R mAb. In all cases, the muscularis was incubated for 30 min at 37°C in complete medium in the presence or absence of BMP2 (10 ng/ml) as indicated. Each data point represents % of pSMAD1/5/8^{+} neurons among total BMPRII^{+} neurons in each visual field; each column summarizes the results from three animals.

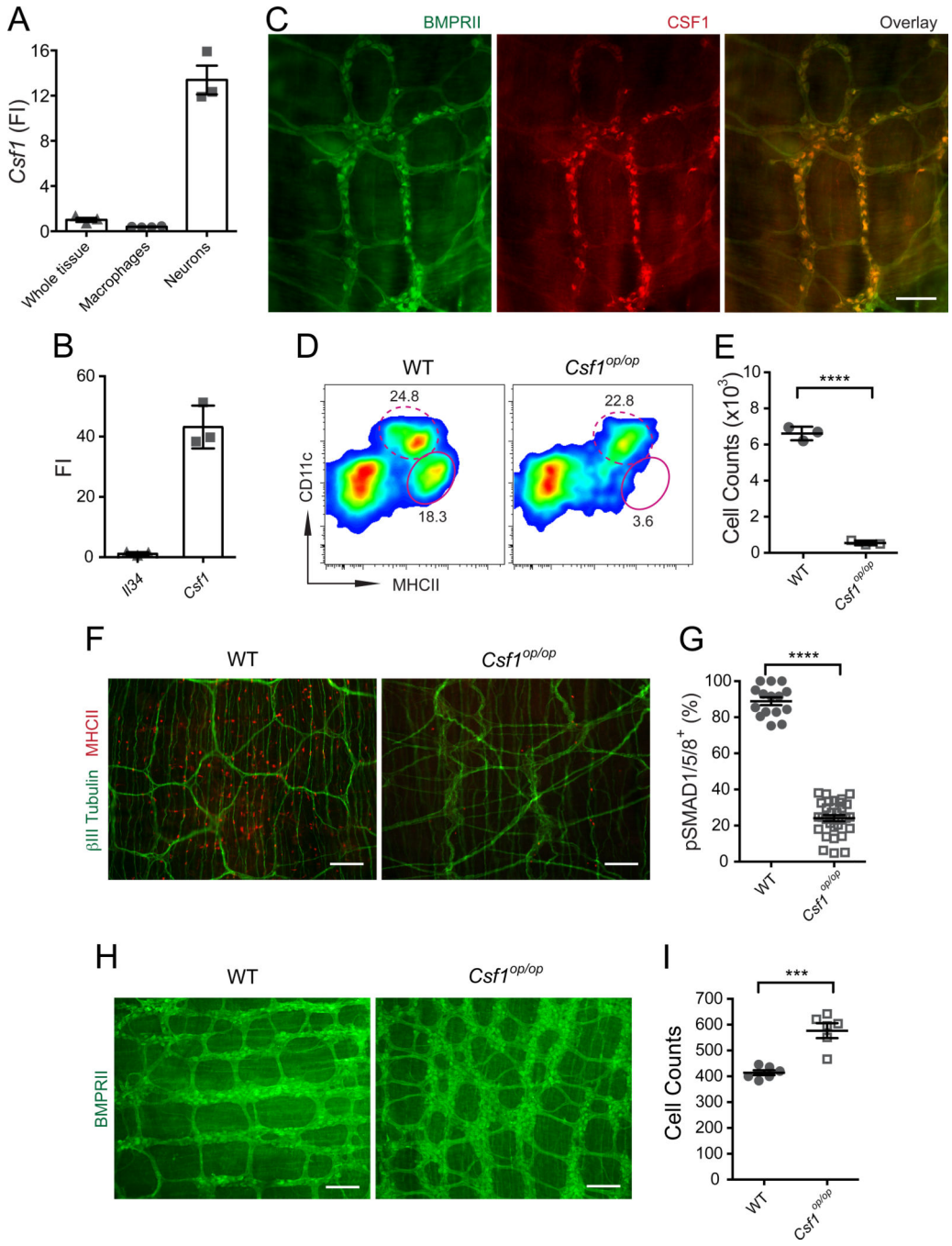

Figure 6. Enteric neurons produce CSF1 required for MM development

(A) *Csf1* gene expression levels measured by qPCR in intact muscularis (whole tissue), macrophages sorted from SB muscularis and cultured primary enteric neurons (FI compared to the "whole tissue"). (B) *Il-34* and *Csf1* relative gene expression levels (FI) measured by qPCR in cultured enteric neurons as compared to *Il-34*. (C) IF analysis of LB muscularis from WT mice stained with anti-BMPRII and anti-CSF1 Abs. Scale bar – 100 nm. (D) FACS plots of whole bowel single cell suspensions from WT mice and their *Csf1*$^{op/op}$ littermates show % of CD11c^{lo}MHCII^{hi} MMs (oval gate, solid line) and CD11c^{hi}MHCII^{hi}

LP phagocytes (oval gate, dashed line). Gated on $CD45^{+}CD11c^{lo/hi}CD11b^{lo/hi}$ cells (E) Absolute MM numbers in the bowel of WT mice and *Csf1*$^{op/op}$ mice quantified by FACS. (F) IF analysis of LB (cecum) muscularis from WT mice and their *Csf1*$^{op/op}$ littermates stained with anti- βIII Tubulin and anti-MHCII Abs. Scale bars – 500 nm. (G) Quantitative summary of the distribution of $pSMAD1/5/8^{+}BMPRII^{+}$ neurons in the LB muscularis from WT and *Csf1*$^{op/op}$ mice. Each data point represents % of $pSMAD1/5/8^{+}$ neurons among total $BMPRII^{+}$ neurons in each visual field; each column summarizes the results from three animals. (H) IF analysis of LB (colon) muscularis from WT and *Csf1*$^{op/op}$ littermates stained with anti-BMPRII Ab. Scale bars – 500 nm. (I) Quantitative summary of the distribution of $BMPRII^{+}$ neurons in the colon of WT and *Csf1*$^{op/op}$ mice. Each data point represents the counts of $BMPRII^{+}$ neurons in each visual field; each column summarizes the results from two animals.

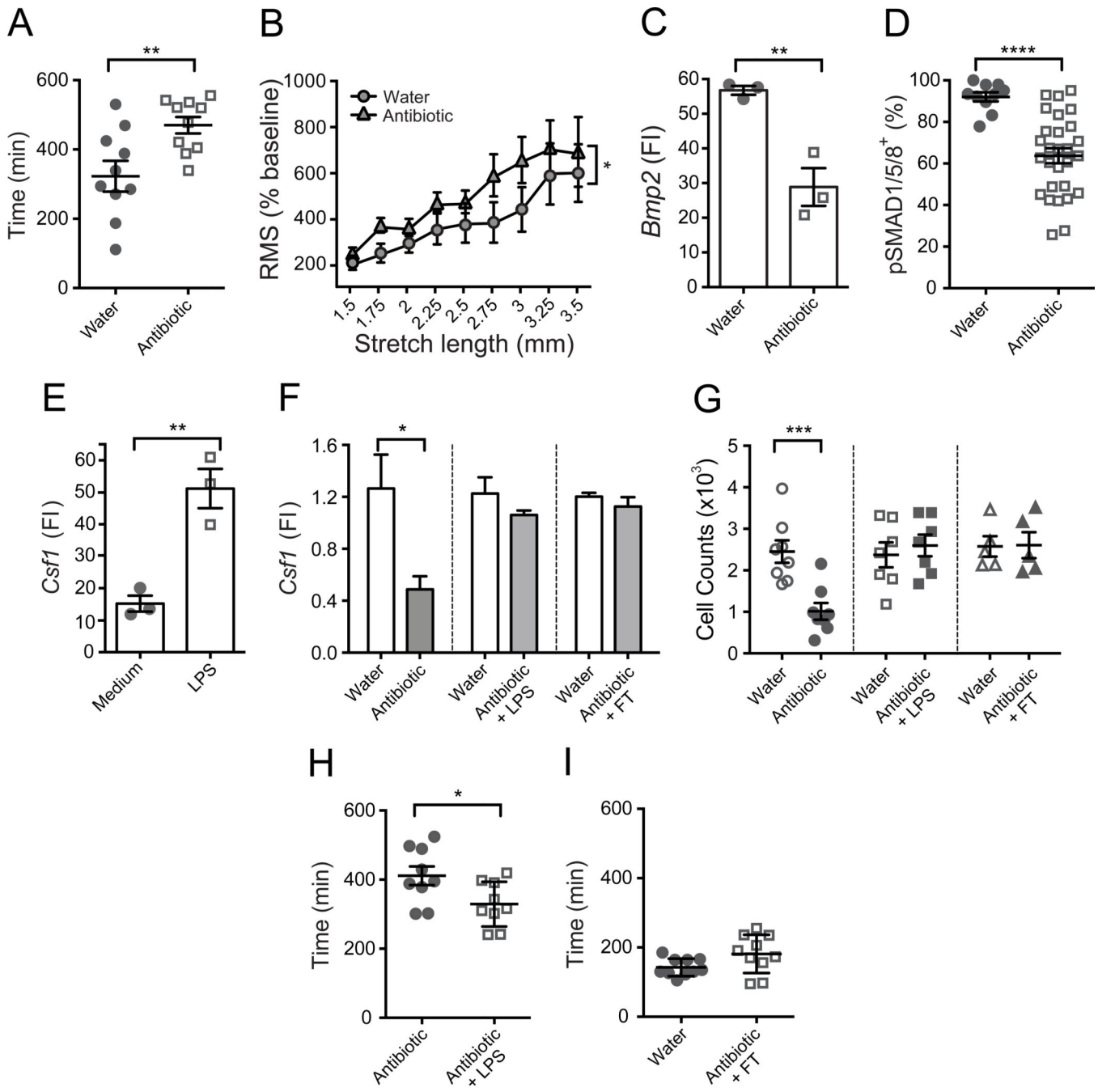

Figure 7. Luminal microbiota regulates intestinal motility and MM-neuronal crosstalk

(A–D) WT mice received antibiotics with drinking water for 4 weeks and control age matched mice received only water. (A) Total GI transit time that represents the time required to expel feces containing carmine red dye measured in antibiotic-treated and control mice. (B) RMS of colonic contraction recordings normalized to baseline (%) at stretch intervals 1.5–3.5 mm. 3 mm colonic rings were obtained from antibiotic-treated and control mice. (C) *Bmp2* relative gene expression levels measured by qPCR in macrophages sorted from separated SB muscularis of antibiotic-treated and control mice. FI – fold increase as compared to *Bmp2* levels in the intact muscularis. Each data point represents qPCR results

obtained from analyzing 50,000 cells after a single sort from 5 mice. Cell sorting from each group was performed in pairs, on the same day and under identical conditions. (D) Quantitative summary of the distribution of pSMAD1/5/8^{+}BMPRII^{+} neurons in the muscularis from antibiotic-treated and control mice. Each data point represents % of pSMAD1/5/8^{+} neurons among total BMPRII^{+} neurons in each visual field; each column summarizes the results from three animals. (E) *Csf1* relative gene expression levels in cultured primary enteric neurons measured by qPCR. Differentiated neurons were cultured with or without 10 ng/ml of LPS for 18 hrs prior to analyses. FI – fold increase as compared to *Csf1* levels in the intact muscularis. Each data point represents qPCR results obtained from an independent neuronal culture. FI – fold increase as compared to *Csf1* levels in the intact muscularis. (F) *Csf1* relative gene expression levels quantified by qPCR in LB muscularis from WT mice were treated with antibiotics for 4 weeks (left), from WT mice treated with antibiotics and 50 μg/ml LPS in drinking water for 4 weeks (middle) and from WT mice 3 weeks after they received fecal transfer (FT) following a 4-week course of antibiotics (right). The data are compared to age matched control mice received only water. FI – fold increase as compared to average *Csf1* levels in the control group received water. (G) Absolute numbers of MMs quantified by FACS in LB from WT mice received antibiotics (left), antibiotics with LPS (middle) and FT following antibiotic treatment (right) as in F. The data are compared to age matched control mice received only water. (H) Total GI transit time in WT mice received antibiotics and 50 μg/ml LPS with drinking water for 4 weeks and age matched mice that received only antibiotics for 4 weeks. (I) Total GI transit time in WT mice 3 weeks after they received FT following a 4-week course of antibiotics and control mice received water.